

RNA interference of LRRK2–microarray expression analysis of a Parkinson’s disease key player

K. Häbig · M. Walter · S. Poths · O. Riess · M. Bonin

Received: 17 September 2007 / Accepted: 2 December 2007 / Published online: 21 December 2007
© Springer-Verlag 2007

Abstract The protein leucine-rich repeat kinase 2 (LRRK2) is a key player in the pathogenesis of Parkinson’s disease (PD). Mutations in the *LRRK2* gene account for up to 10% of all autosomal dominant forms of familiar and for approximately 1–3% of sporadic PD patients. Although the LRRK2 protein has many functional domains like a leucine-rich repeat domain, a Roc-GTPase domain, a kinase domain of the tyrosine kinase-like subfamily and multiple protein interaction domains (armadillo, ankyrin, WD40), the exact biological role of LRRK2 in the human brain is elusive. To gain more insight into the biological function of this protein, we monitored the changes in the expression profiles of SH-SY5Y cells, a dopaminergic neuroblastoma cell line, induced by a depletion of *LRRK2* levels by RNA interference (RNAi) with Affymetrix U133 Plus 2.0 microarrays. A total of 187 genes were differentially regulated by at least a 1.5-fold change with 94 transcripts being upregulated and 93 transcripts being downregulated compared to scrambled control siRNA transfected cells. Key players of the interaction networks were independently verified by qRT-PCR. The differentially expressed gene products are involved in axonal guidance, nervous system development, cell cycle, cell growth, cell differentiation, cell communication, MAPKKK cascade, and Ras protein signal transduction. Defined gene expression networks will now serve to look more closely for

candidates affected by LRRK2 reduction and how they might be altered in other forms of familial or sporadic PD.

Keywords LRRK2 · Microarray analysis · Parkinson’s disease · PARK8 · RNA interference

Introduction

Although Parkinson’s disease (PD) is the second most common neurodegenerative disease [1] the underlying pathogenesis is still widely elusive. Genetic analyses of familial forms of PD lead for the first time to a specific chance to study alterations causative for PD. A protein that plays an important role in this disease is the leucine-rich repeat kinase 2 (LRRK2, PARK8) [2]. Until now, more than 20 mutations were found in *LRRK2* accounting for approximately 5–10% of familial PD and up to 3% of sporadic PD cases, both indistinguishable in their pathological hallmarks [3–12]. Therefore, clarifying of the biological function of the 280 kDa multidomain protein LRRK2 will give new insights in the pathogenesis of PD.

The LRRK2 protein consists of a number independent protein domains, and most of the PD associated mutations affect nearly every predicted catalytic and protein–protein interaction domain [13]. One of the known protein–protein interaction domains of LRRK2 is the leucine-rich repeat (LRR) domain [13, 14]. This repeat is flanked by a Rho/Ras-like GTPase domain (termed Roc, for Ras in complex proteins) followed by an associated C-terminal of Roc (COR) domain, which function is still unknown [13]. The Roc-GTPase domain of LRRK2 resembles most closely the Rab (Ras-related in brain) family of GTPases [13], which are central regulators of vesicle formation, actin- and tubulin-dependent vesicle movement, and membrane fusion

Electronic supplementary material The online version of this article (doi:10.1007/s10048-007-0114-0) contains supplementary material, which is available to authorized users.

K. Häbig · M. Walter · S. Poths · O. Riess · M. Bonin (✉)
Department of Medical Genetics, Microarray Facility,
University of Tübingen,
Calwerstrasse 7,
72076 Tübingen, Germany
e-mail: Michael.Bonin@med.uni-tuebingen.de

[15]. C-terminal of the Roc-GTPase and its COR domain LRRK2 contains a protein kinase domain. Additionally, to the previous mentioned LRR domain, there is weak prediction for a single WD40 repeat at the C-terminal end of LRRK2, namely the WD40 domain [16]. WD40 repeats could serve as scaffold for protein interactions and these interactions can occur simultaneously with several different proteins [17]. The N-terminal side of LRRK2 contains 14 evolutionary conserved repeats with unknown function [16]. Although the domain structure of LRRK2 is well known, the elucidation of the biological function of the protein is still in the early stages. By means of RNA interference (RNAi; for a review see [18]), we reduced the mRNA level of *LRRK2* in the human dopaminergic neuroblastoma cell line SH-SY5Y. The examination of the alterations in the expression profile (with Affymetrix Human Genome U133 Plus 2.0 Arrays) provoked by the loss of *LRRK2* provided us with new insights in the signaling pathways of the protein.

Material and methods

Cell culture and RNA interference

Human SH-SY5Y cells were maintained in D-MEM medium (Invitrogen) supplemented with 15% fetal bovine serum and penicillin–streptomycin.

RNAi of *leucine-rich repeat kinase 2* (*LRRK2*) was performed with two different chemical synthesized siRNAs against *LRRK2* (Qiagen) and control siRNA (Qiagen) with random sequence not present in the human genome. The effect of these siRNA (listed in Table 1) was determined with qRT-PCR.

All transfection experiments were performed in independent triplicates with the Cell Line Nucleofection Kit V (Amaxa) according to the manufactures protocol. For the electroporation with program G-04, we applied 2×10^6 cells and 2 μ g siRNA.

RNA isolation and cDNA preparation

Total RNA of transfected cells (48h after RNAi treatment) was isolated using the RNeasy Mini Kit (Qiagen) including

a DNase digest on the column with RNase-Free DNase Set (Qiagen). The RNA quality was controlled by Lab-on-Chip-System Bioanalyser 2100 (Agilent), and the concentration was determined using a BioPhotometer (Eppendorf).

cDNA synthesis was performed with 1 μ g of total RNA using the QuantiTect Reverse Transcription Kit (Qiagen). For examination of genomic DNA contamination, we included a RT-negative control.

Microarray analysis

Microarray analysis was performed using an Affymetrix platform and the according materials and protocols. Fragmented and labeled cRNA of control siRNA treated cells and siLRRK2-1 treated cells (triplicates of each condition) were applied to the hybridization using the Human Genome U133 Plus 2.0 Array (Affymetrix). Data analysis was performed with ArrayAssist 4.0 (Stratagene) with a low stringency filtering scheme of 1.5-fold change in expression level and *p* value of less than 0.05 after GC-RMA normalization of all data sets.

Generating of functional categories and pathway analysis

The probeset IDs of the differentially expressed transcripts were integrated in BiblioSphere (Genomatix software GmbH), and Gene Ontology categories were identified for annotated genes. This software facilitates the categorization of the genes to biological processes, while one gene could be associated to more than one functional category. For each GO category, a Z-score is calculated, which indicates how far and in what direction that term deviates from its distribution's mean, expressed in units of its distribution's standard deviation. The significance of the GO group increases with higher levels of the Z-score and we choose 3.9 as cut off.

Gene regulation networks were generated using Ingenuity pathways analysis software (ingenuity® systems, www.ingenuity.com). The data set with differentially regulated transcripts and corresponding expression values was uploaded into the application. Each gene identifier was mapped to its corresponding gene object in the ingenuity pathways knowledge base. The genes were overlaid onto a global molecular network developed from information contained in the ingenuity pathways knowledge base. Networks of these focus genes were then algorithmically generated based on their connectivity. All edges are supported by at least one reference from the literature, from a textbook, or from canonical information stored in the ingenuity pathways knowledge base. The functional analysis was also done with this software. Genes from the microarray dataset that met the fold change cutoff of 1.5 and that were associated with a canonical pathway in the ingenuity path-

Table 1 Sequences of transfected siRNA (Qiagen)

siRNA	Sequence (5'-3')
siLRRK2-1	CTCGTCGACTTATACGTGTAA
siLRRK2-2	CAGAAATTCATCATAAGCTAA
Control siRNA	AATCTCCGAACGTGTACGCT

Table 2 Oligonucleotides for the qRT-PCR

Transcript	QuantiTect Primer Assay	Forward sequence	Reverse sequence
<i>CHRM3</i>		TGTCACTGTTTTGCATCCTTG	CAAAGGCGAGGTTGTA CTGTT
<i>CIT</i>		CAGTCAGCCTGCTCTGATGA	GAAGGCTGGAGCTCCTGTAA
<i>CSNK1G1</i>		CCTATGATTGGGTTGGGAGA	GCTTTCTCGAGTTATTGCAGATG
<i>CUL3</i>		AGAAAGAAGATGCAGCACAATG	ACA ACTGGACTTGGTAAGAATCG
<i>CXCR4</i>		AAATGGGCTCAGGGGACTAT	GTAGATGGTGGGCAGGAAGA
<i>GNAO1</i>		CCTTTGACCATCTGCTTTCC	TGCTTTCAAATTGTGCTTGG
<i>ITGB5</i>		AGTTTCAGAGCGAGCGATCC	CCACAGTGTGCGTGGAGATA
<i>LRRK2</i>		ATGATGACAGCACAGCTAGGA	AAACGGTCAAGCAAGATTGTA
<i>NQO1</i>		GATCCACGGGGACATGAAT	TGTCAGTTGAGGTTCTAAGACTTG
<i>PDHB</i>		GGTTTCCCATTC AAGACCTG	TGGTTTCCATGTCCATTGGT
<i>SCG5</i>		TGAAGGGAGGAGAGAGACGA	GACAGACTTCTTTGCAACAACA
<i>ARHGEF7</i>	QT01011913		
<i>CALB1</i>	QT00011823		
<i>CAMKK2</i>	QT00040033		
<i>CDC42</i>	QT00066528		
<i>FGF2</i>	QT00047579		
<i>INHBA</i>	QT00201586		
<i>MYC</i>	QT00035406		
<i>SDHA</i>	QT00059486		

ways knowledge base were considered for the analysis. The significance of the association between the data set and the canonical pathway was measured in two ways: (1) A ratio of the number of genes from the data set that map to the pathway divided by the total number of genes that map to the canonical pathway is displayed, and (2) Fischer's exact test was used to calculate a *p* value determining the probability that the association between the genes in the dataset and the canonical pathway is explained by chance alone.

Quantitative real-time PCR

The quantitative real-time PCR (qRT-PCR) was performed on the LightCycler 480 System (Roche) in 384-well format. Specific QuantiTect Primer (Qiagen) or Primer designed with the Primer3 Software (http://frodo.wi.mit.edu/cgi-bin/primer3/primer3_www.cgi) spanning an Exon–Exon boundary were applied for amplification (listed in Table 2). We used 10 μ l reaction volume containing 1 μ l of 1:5 diluted cDNA and the QuantiTect[®] SYBR[®] Green PCR Kit (Qiagen) with PCR settings according to the manufactures protocol. Melting curves were generated at the end of the run. Standard curves of each amplified gene were created, to obtain the PCR efficiency. The *cp*-values of the genes were detected by the LightCycler 480 Software release 1.2.0.0625 applying the second derivative maximum method. For data analysis, the best out of two reference genes (*SDHA* and *PDHB*) was identified by the GeNorm algorithm implemented in the qBASE application [19, 20] and subsequently used for normalization and calculation of the relative expression with REST-384[©] version 2 [21, 22].

Results

Efficiency of RNAi

RNAi downregulation of *LRRK2* was performed with two distinct siRNA as well as a nonhomologous control siRNA in SH-SY5Y cells. Downregulation of *LRRK2* mRNA was confirmed with qRT-PCR. Control siRNA did not result in a change in *LRRK2* expression level relative to untransfected cells whereas electroporation with siLRRK2-1 leads to an obvious reduction of *LRRK2* mRNA level to a relative expression of 0.25 (Fig. 1). However, the relative expres-

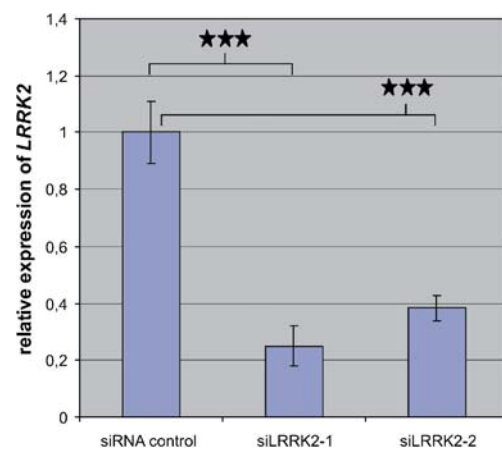


Fig. 1 Reduction of LRRK2 expression by RNAi. SH-SY5Y cells were transfected with two different siRNAs and expression was determined by qRT-PCR. The analysis was done in independent replicates (error bias=SEM). *PDHB* was used as reference gene. ****p* value \leq 0.001

sion of *LRRK2* in cells treated with siLRRK2-2 achieved only 0.38. Thus, siLRRK2-1 was identified as the most effective mediator of the RNAi of *LRRK2* and subsequent experiments were performed using this siRNA.

Microarray analysis

RNAi of *LRRK2* is likely to influence the expression level of transcripts, associated with the biological function of *LRRK2*. To identify changes in the expression level of putative interactors, we performed a microarray analysis with Affymetrix Human Genome U133 Plus 2.0 microarrays. The analysis by means of the ArrayAssist 4.0 software identified 187 transcripts differentially regulated between triplicates of control siRNA and siLRRK2-1 transfected SH-SY5Y cells. There were 94 of these transcripts upregulated and 93 transcripts downregulated with a fold change of at least 1.5 and a *p* value of less than 0.05. A complete list of all differentially regulated genes in this RNAi experiment is provided in the Supplementary material 1.

Identification of biological context-network analysis

GO categories

The BiblioSphere software (Genomatix software GmbH) was used to assort the 187 differentially expressed transcript to gene ontology (GO) categories of biological

processes. A total of 131 of the 187 differentially expressed transcript IDs could be mapped in the analysis, and 65 are alignable with GO categories (Fig. 2). The overview about the differentially expressed transcripts in the influenced 16 GO categories could be found in the Supplementary material 2.

We examined four differentially regulated transcripts which are associated with axonal guidance and this category obtained the highest Z-score with 7.1. In the biological category “nervous system development” 14 genes were disregulated with the second highest Z-score of 6.7. Furthermore, four transcripts (Z-score 6.6) within the biological processes “cell cycle arrest” and five transcripts (Z-score 5.9) of “regulation of cell growth” showed a different expression compared to cells transfected with control siRNA. Downregulation of *LRRK2* influenced also the expression profile of six transcripts (Z-score 5.9) related to “cell projection morphogenesis”. Additionally, 8 “cell motility genes” (Z-score 5.2) and 14 “anatomical structure morphogenesis genes” (Z-score 5) were disregulated. The biological process “cell communication” highlighted the highest number of differentially regulated transcripts (30, Z-score 4.8) in our microarray experiments. Accessorily, 6 transcripts (Z-score 4.4) of “regulation of multicellular organismal process”, 4 transcripts (Z-score 4.3) of the GO category “MAPKKK cascade” and 26 transcripts (Z-score 4.3) of “developmental process” appeared disregulated in *LRRK2* repressed cells. The analysis point out two GO categories with a Z-score of 4.1, these include 17

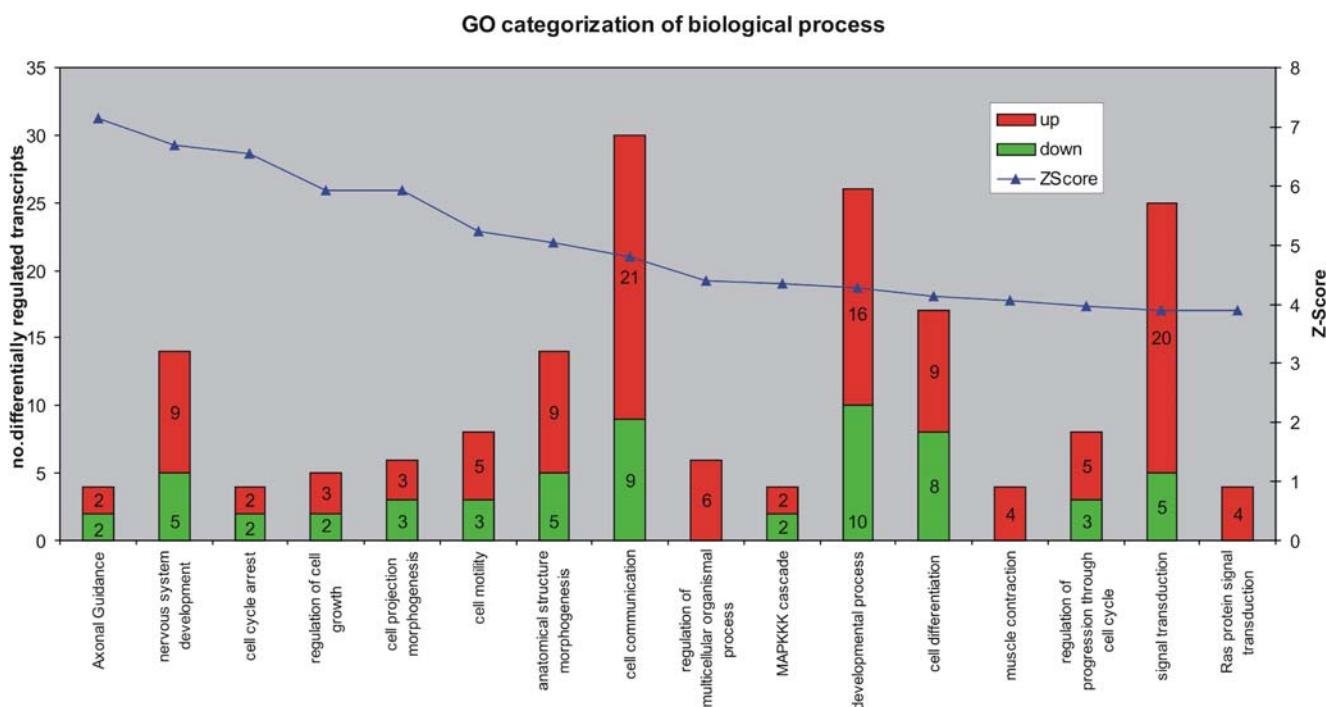


Fig. 2 Differentially expressed genes were grouped by GO functional categories of biological processes. The numbers of differentially expressed transcripts of one GO category are shown as bar and the specific Z-score is shown as rhomb

differentially regulated transcripts of “cell differentiation” and 4 differentially regulated transcripts of “muscle contraction”. Furthermore, we examined the regulation of 8 transcripts (Z-score 4) associated with “regulation of progression through cell cycle” and 25 transcripts (Z-score 3.9) of “signal transduction”. In the GO category “Ras protein signal transduction” four genes (Z-score 3.9) appeared differentially upregulated in *LRRK2* repressed cells.

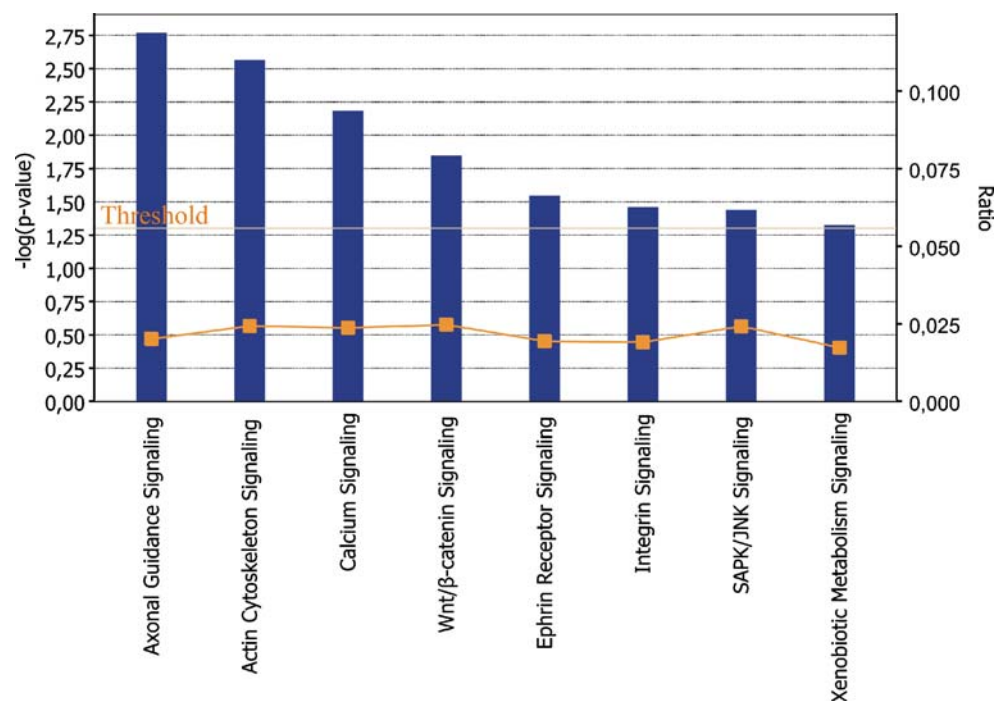
Ingenuity canonical pathway analysis

By means of the ingenuity pathways analysis software (Ingenuity Systems), we analyzed the canonical pathways which are affected by the repression of *LRRK2* with RNAi (Fig. 3). A total of 151 of the 187 differentially expressed transcript IDs could be mapped in the analysis and 84 are alignable with functions. We defined a deregulation of transcripts in nine different canonical pathways with a $-\log(p \text{ value}) \geq 0.98$ and a ratio ≥ 0.017 . Affected pathways included axon guidance signaling, actin cytoskeleton signaling, calcium signaling, Wnt/ β -catenin signaling, ephrin receptor signaling, integrin signaling, SAPK/JNK signaling, and Xenobiotic metabolism.

Since one gene could be part of various pathways, we identified the differentially upregulated gene *CDC42* (cell division cycle 42, fold change 2.47, p value 0.01) as major gene participating in five of the nine identified canonical pathways. Among these are axon guidance signaling, actin cytoskeleton signaling, ephrin receptor signaling, integrin

signaling and SAPK/JNK signaling. Additionally, the upregulated guanine exchange factor *ARHGEF7* (Rho guanine nucleotide exchange factor 7, 2.01, 0.02) has a key position in integrin signaling, actin cytoskeleton signaling and axon guidance signaling. The downregulation of *CUL3* (cullin 3, -1.77 , 0.04) and *MGMT* (O-6-methylguanine-DNA methyltransferase, -2.70 , 0.001) as well as the upregulation of *NQO1* [NAD(P)H dehydrogenase, quinone 1, 1.74, 0.03] and *PPP2R2A* (protein phosphatase 2 regulatory subunit B, 1.59, 0.0003) are features of the impaired xenobiotic signaling. The protein phosphatase subunit is a component of the canonical Wnt/ β -catenin signaling pathway. In this pathway, *CSNK1G1* (casein kinase 1 gamma 1, 1.86, 0.02), *DVL2* (dishevelled dsh homolog 2, 1.53, 0.003), and *GNAO1* (guanine nucleotide binding protein alpha activating activity polypeptide O, 1.76, 0.004) are misregulated. Another protein phosphatase subunit *PPP1R12B* (protein phosphatase 1 regulatory subunit 12B, 2.09, 0.002), which appeared to be upregulated in the microarray experiment, is part of the integrin signaling cascades. The key player of this canonical pathway is the upregulated integrin *ITGB5* (integrin beta 5, 1.83, 0.0007). The change in expression profile in ephrin signaling is characterized by the upregulation of *GNAO1*, *CDC42*, *EFNB2* (ephrin-B2, 1.55, 0.0003) and the downregulation of *CXCR4* (chemokine C-X-C motif receptor 4, -2.02 , 0.0003). All of these genes participate also in axonal guidance in addition to *ARHGEF12* (Rho guanine nucleotide exchange factor 12, 1.56, 0.009), *BMP2* (bone morphogenetic protein 2, 1.57, 0.04), *SEMA4F* (sema

Fig. 3 Analysis of canonical pathways affected by *LRRK2* RNAi. The analysis was done with Ingenuity Pathways Analysis software. Fischer’s exact test was used to calculate a p value (shown as bars) determining the probability that each biological function assigned to the network is due to chance alone. The ratio (shown as squares) represents the number of differentially expressed genes in a given pathway divided by total number of genes that make up that canonical pathway



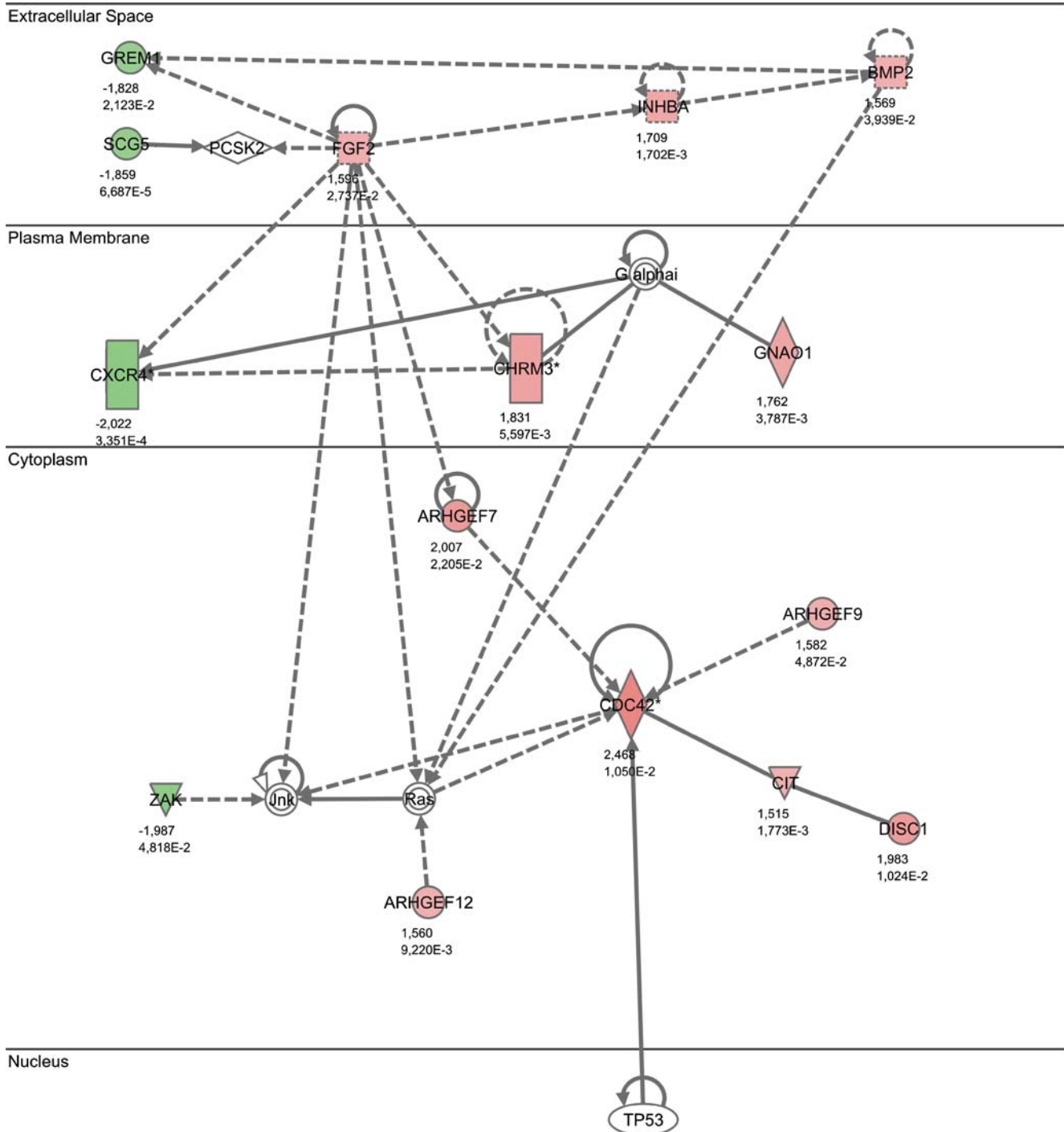


Fig. 4 Network 1 of differentially regulated transcripts with the key players FGF2 and CDC42. The gene regulation network, established with the ingenuity pathways analysis software contains 20 genes with 11 genes being upregulated (red icons) and 4 downregulated genes

(green icons). Five genes are implemented in the network to complete the interactions. The fold change of the regulation in the microarray analysis as well as the *p* value of the significance analysis is listed below the gene symbols

domain 4F, -1.61, 0.002), and the previous mentioned gene *ARHGEF7*. Five genes are upregulated in calcium signaling cascades, namely *CACNA1G* (calcium channel voltage-dependent, alpha 1G subunit, 1.59, 0.004), *CAMKK2* (calcium/calmodulin-dependent protein kinase kinase 2 beta, 1.83, 0.05), *TPM1* (tropomyosin 1, 1.79, 0.03),

TPM3 (tropomyosin 3, 1.62, 0.013), and *TPM4* (tropomyosin 4, 1.62, 0.0009). The dysregulation of the actin cytoskeleton signaling is characterized by the upregulation of *CHRM3* (cholinergic receptor muscarinic 3, 1.88, 0.0007) and *FGF2* (fibroblast growth factor 2, 1.6, 0.03) in addition to *ARHGEF7*, *CDC42*, *PPP1R12B*, and

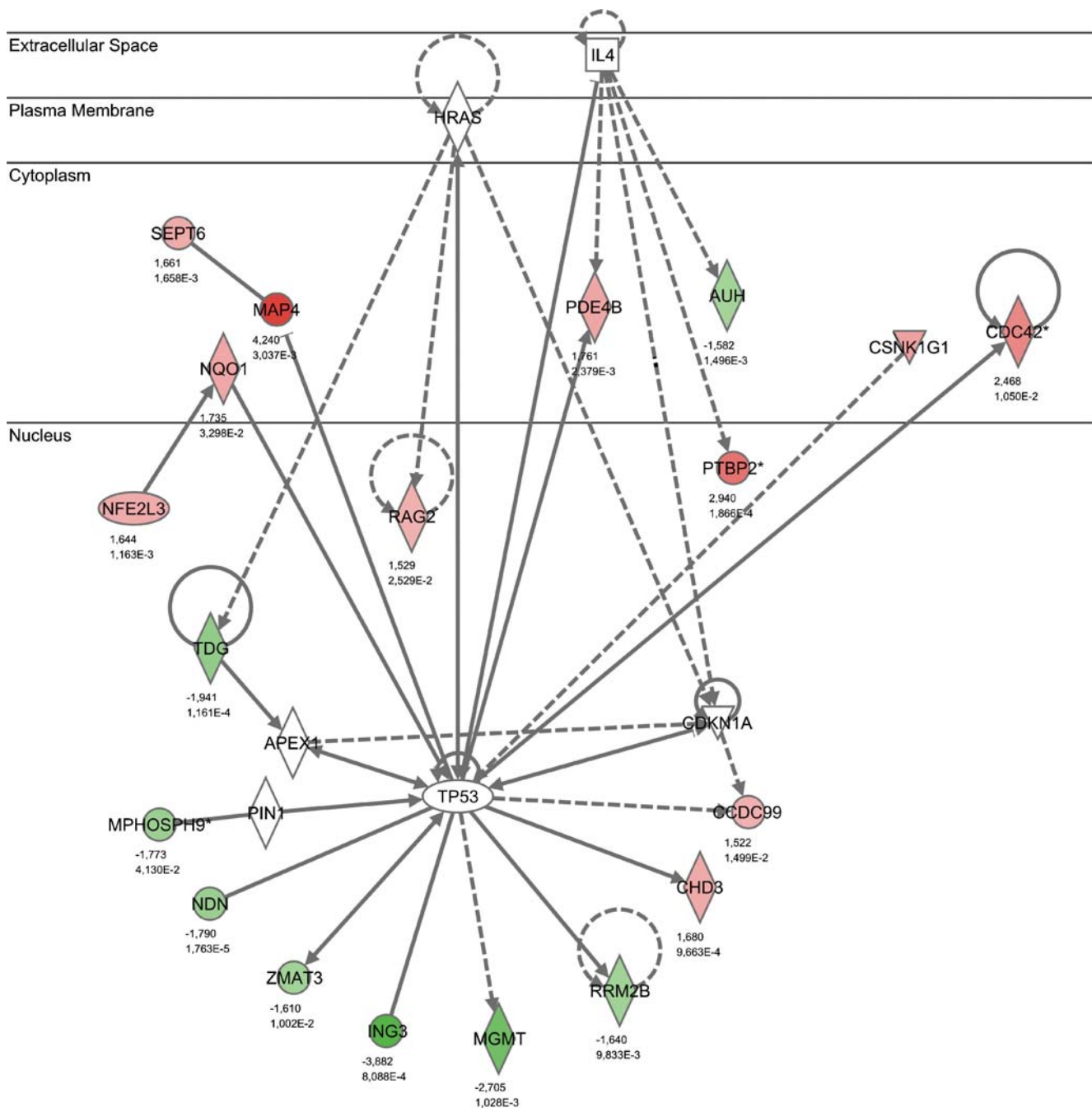


Fig. 5 Network 2 of differentially regulated transcripts with the key player TP53. The gene regulation network, established with the ingenuity pathways analysis software contains 25 genes with 11 genes being upregulated (*red icons*) and 8 downregulated genes (*green*

icons). Six genes are implemented in the network to complete the interactions. The fold change of the regulation in the microarray analysis as well as the *p* value of the significance analysis is listed below the gene symbols

ARHGEF12, which participates in other pathways too. Although only three genes are misregulated in the SAPK/JNK canonical pathway, they reached significance over the $-\log(p \text{ value})$ threshold (1.3). In this pathway, *CDC42* and *CHRM3* were upregulated and the kinase *ZAK* (sterile alpha motif and leucine zipper containing kinase *AZK*, -1.99 , 0.048) was downregulated.

Ingenuity network analysis

Other software tools of the ingenuity pathways analysis software (Ingenuity Systems) were used to examine the connection within the differentially expressed transcripts independently of canonical pathways. 88 of 151 differentially expressed transcript IDs, which could be mapped in the

Extracellular Space

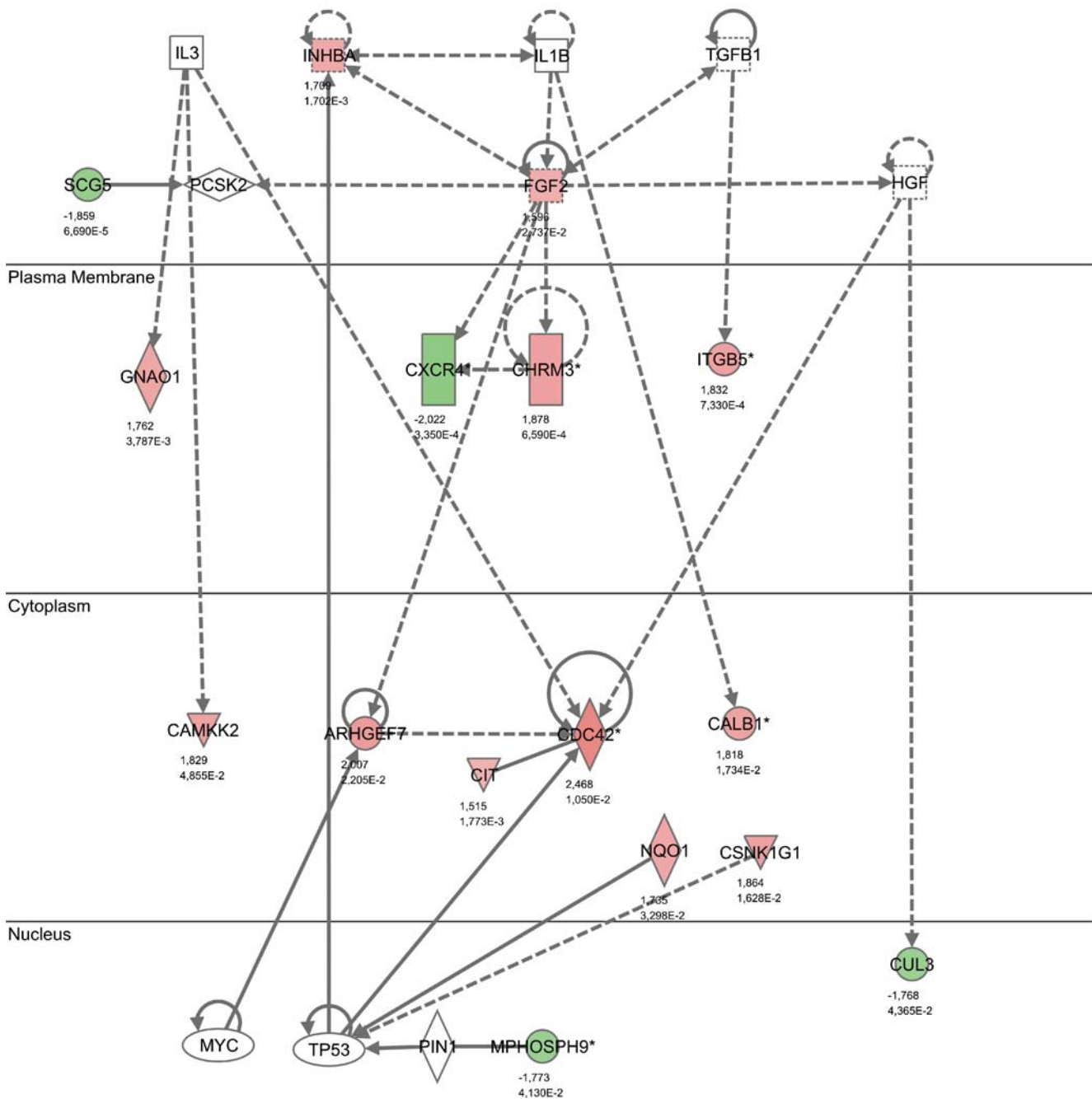


Fig. 6 Network of differentially expressed transcripts used for validation in qRT-PCR. The gene regulation network, established with the ingenuity pathways analysis software contains 24 genes with 12 genes being upregulated (red icons) and 4 downregulated genes (green icons). Eight genes are implemented in the network to complete

the interactions. The fold change of the regulation in the microarray analysis as well as the *p* value of the significance analysis is listed below the gene symbols. Because of complexity only some of the known gene to gene interactions are shown. 16 of the shown transcripts were used for qRT-PCR validation

ingenuity analysis are alignable with networks. In Figure 4, a network of differentially regulated genes detected by reduction of *LRRK2* with RNAi around the upregulated genes *CDC42*, *ARHGEF7*, and *FGF2* is shown. In this pathway, the influence of *FGF2* on proteins with G-protein coupled

receptor activity in the plasma membrane *CHRM3* and *CXCR4* is highlighted. In extracellular space, *SCG5* (secretory granule neuroendocrine protein 1, -1.86, 0.00007), *INHBA* (inhibin beta A, 1.71, 0.002), *GREM1* (gremlin 1, -1.83, 0.02), and *BMP2* are misregulated, all of them directly

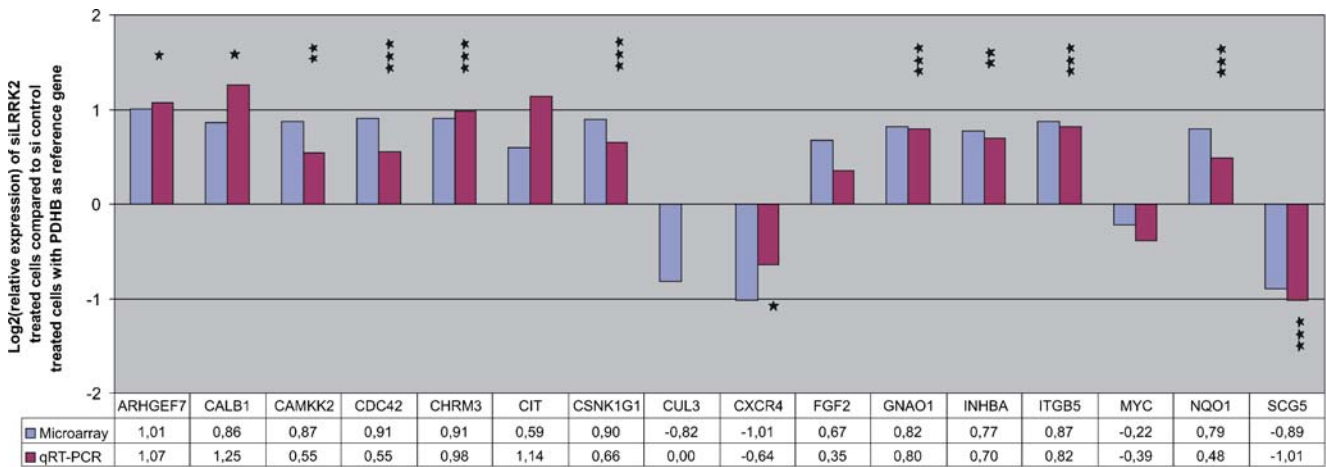


Fig. 7 qRT-PCR results of array validation. The same type of regulation was observed for all transcripts except CUL3. The signal log ratio (Log₂ of relative expression) for the microarray analysis and

the qRT-PCR validation is given below the graph for each gene. **p* value ≤ 0.05. ***p* value ≤ 0.01. ****p* value ≤ 0.001

or indirectly connected with *FGF2*. The regulation cascades around *FGF2* are also associated with genes in the cytoplasm like the upregulated gene *ARHGEF7*. The upregulation of this guanidine exchange factor is in concordance with the upregulation of *CDC42*, which is in connection with the upregulation of another guanidine exchange factor *ARHGEF9* (*Cdc42* guanine nucleotide exchange factor 9, 1.58, 0.048). Additionally, *ARGHEF12*, which is in connection to *CDC42* via the unregulated gene Ras, is also upregulated. The network is also characterized by the regulation of two different kinases. The rho-interacting, serine/threonine kinase 21 (*CIT*, 1.52, 0.002) is upregulated and in relationship to *CDC42*. The MAPKKK *ZAK* which is connected over the unregulated *JNK* with *CDC42* is downregulated. The prominent key player of this network *CDC42* is in dependency to *TP53*. We could establish a network around *TP53* (Fig. 5) highlighting seven downregulated genes (*MGMT*, *RRM2B*, *MPHOSPH9*, *ING3*, *NDN*, *ZMAT3*, *TDG*) and seven upregulated genes (*NQO1*, *MAP4*, *PDE4B*, *CSNK1G1*, *CCDC99*, *CHD3*, *CDC42*). Accessorily to the upregulation of *NQO1*, its expression regulating gene *NFE2L3* (nuclear factor erythroid-derived 2-like 3, 1.64, 0.001) is upregulated too. The same effect could be seen by *MAP4* (microtubule-associated protein 4, 4.24, 0.003) and its interaction partner *SEPT6* (septin 6, 1.66, 0.002). Additionally, to *PDE4B* (phosphodiesterase 4B, 1.76, 0.002) there are two more differentially regulated genes with relation to *IL4* named *PTBP2* (polypyrimidine tract binding protein 2, 2.94, 0.0002) and *AUH* (AU RNA binding protein/enoyl-Coenzyme A hydratase, -1.58, 0.001).

Validation of the microarray experiment

We choose 16 key players of the interaction networks for independent verification by qRT-PCR. These transcripts are in relation to each other as demonstrated in a validation pathway (Fig. 6). We analyzed the transcript level of *SDHA*

and *PDHB* with qRT-PCR and identified *PDHB* as the best reference gene with the GeNorm algorithm. Therefore, transcript levels of *PDHB* were used for calculation of relative expression of the target genes. We could validate 14 of 16 genes, except of *CUL3* and *MYC*. So the results of the qRT-PCR (Fig. 7) showed 87.5% validation efficiency in comparison to the expression data of the microarray experiment. The microarray expression of *MYC* was not significantly impaired in *LRRK2* repressed cells, but with qRT-PCR measurement, we found a minor reduction of this gene. Examining the expression of *FGF2*, we detected a small upregulation in the microarray analysis and were also able to validate this in qRT-PCR although with low value.

Discussion

The biological function of *LRRK2*, a protein implicated in Parkinson’s disease, is still elusive [23]. RNA interference was performed to repress the *LRRK2* mRNA expression in SH-SY5Y cells. We used two different synthetic siRNAs; however, only one siRNA (siLRRK2-1) was able to knock down *LRRK2* by 75%. Differences of the *LRRK2* mRNA target sequences might explain the discrepancies of siRNA efficiency [24]. The repression of *LRRK2* on mRNA did not reflect an unspecific effect of the transfection procedure or siRNA treatment, since control siRNA provoked no effect.

Overall, the microarray analysis resulted in 187 differentially expressed transcripts, characterized by at least 1.5-fold change and a *p* value < 0.05 with 94 transcripts being up-regulated and 93 transcripts being downregulated. Fourteen of sixteen differentially expressed transcripts (87.5%) were confirmed by qRT-PCR, which is in accordance with quotas mentioned in literature [25].

By means of the analysis of the GO categories, the canonical pathways and the networks impaired by the

reduction of *LRRK2*, we could clearly demonstrate the influence in GTPase mediated signal transduction. The upregulated Ras related GTP-binding protein *CDC42* is implicated in the regulation of cell morphology, motility and cell cycle progression [26, 27]. It is a key player in five identified canonical pathways and in our established network 1. Through the Rho GTPases like *RHO*, *RAC*, and *CDC42*, the regulation of actin-based motility occurs, which is critical for nervous system development [28]. Previous studies highlighted the role of *LRRK2* in regulating neurite process morphology and pointed out that the downregulation of *LRRK2* with short hairpin RNA vectors results in a prominent increase in neurite length [29]. GTPases can switch between “inactive” GDP bound and “active” GTP bound conformations. The nucleotide exchange is catalyzed by GDP/GTP exchange factors (GEF), converting the GTPase in a conformation that can interact with downstream effector proteins [15]. The downregulation of *LRRK2* results, additionally to the upregulation of *CDC42*, in the upregulation of three different guanidine exchange factors (*ARHGEF* 7, 9, 12). Additionally, the guanine nucleotide binding protein *GNAO1* as well as *RGS20*, which has GTPase activator activity, are upregulated. Since *LRRK2* has a Roc-GTPase domain [13], its function could be closely related with guanidine exchange factors and GTP binding proteins.

Furthermore, West et al. [30] showed that the *LRRK2* GTPase activity functions independently of the kinase activity, but the kinase activity requires the GTPase activity, and both are required for neurotoxicity of *LRRK2*. They also suggest that *LRRK2* requires co-factors for the binding and hydrolysis of nucleotides in the GTPase domain, reinforcing the analysis of *ARHGEF* 7, 9 and 12 as possible mediators.

Recent studies highlighted that overexpression of *LRRK2* with autosomal-dominant mutations leads to disinhibited kinase activity, a reduction in neuron process length and complexity and the accumulation of tau-positive inclusion with lysosomal characteristics [29]. More detailed analysis in the kinase signaling cascades pointed out that mutations linked to familial PD in *LRRK2* did not obviously perturb the MAPK pathway [30]. However, we could show upregulation of *CHRM3* and downregulation of *ZAK* (a MAPKKK), both implemented in SAPK/JNK canonical pathways [31]. In addition, *CAMKK2* is upregulated participating in MAPKKK cascades [32, 33]. Especially worth mentioning is the upregulation of *CIT* in our RNAi experiment. This protein has accessorially to its kinase activity a GTPase regulating activity [34] suggesting it could have relevance in the pathways influenced by *LRRK2* reduction.

Recent studies discussed the influence of p53 protein level in the degeneration of the nigrostriatal dopaminergic neurons in parkinsonian brain [35] and the impact of the phosphorylation of p53 on cell death in dopaminergic neurons [36]. The protein p53 is known to induce cell cycle

arrest or apoptosis by differential transcription of target genes and through transcription independent apoptotic function [37]. By means of our network 2, we demonstrate the effect of the loss of *LRRK2* on p53 signaling cascades. We found 12 misregulated transcripts with direct and 7 misregulated genes with indirect contact to *TP53*. In response to *LRRK2* reduction, the cell cycle influencing transcripts *CDC42*, *MAP4*, *SEPT6*, *MPHOSPH9*, and the apoptosis related transcripts *NQO1*, *CSNK1G1*, *RAG2*, *ZMAT3*, *MGMT*, *NDN* as well as *ING3* are effected in their expression level. By means of the supplied analysis, we highlighted the impact of the loss of *LRRK2* on p53 signaling, which is in relation to the previously mentioned publications [35–37].

Considering the interaction partners of *LRRK2* which were identified by Dächsel et al. [38], four groups of interacting proteins could be found. They are chaperone proteins, proteins linked to cytoskeleton and trafficking, proteins associated with phosphorylation, and others like eukaryotic translation initiation factors. Among them are the chaperone proteins HSPA9 and HSPA8 known as binding partners of p53 [39, 40].

The Protein p53 decreases the expression of *HSP90AB1* and *HSP90AA1* [41, 42] both likewise interaction partners of *LRRK2* [38]. Additionally, p53 can regulate the expression of *FGF2* and vice versa [43, 44]. This upregulated growth factor is associated with actin cytoskeleton signaling [45]. It can regulate the expression of *VIM* [46], which is a potential interaction partner of *LRRK2* [38] and also participating in cytoskeleton signaling [47].

Additionally to *FGF2*, there is an upregulation of *MAP4*, *TPM1*, *TPM3*, *TPM4*, *KIF21B* and a downregulation of *ATG4A*, all of these affecting cytoskeleton signaling. In detail, *MAP4* is a positive regulator of microtubule stabilization [48], *ATG4A* has microtubule binding opportunities [49] and *KIF21B* can influence microtubule based movement [50]. Interestingly, *LRRK2* was recently shown to phosphorylate the actin-binding proteins moesin, esrin, and radixin [51]. The *LRRK2* RNAi-regulated TPM proteins found here also have actin-binding activity [52], making them obvious candidate substrates of *LRRK2*. These results enforce the hypothesis that the biological function of *LRRK2* is closely related to actin based motility, which is critical for nervous system development [28]. This theory is supported by the regulation of genes associated with neurogenesis and neurotransmitter catabolism and differentiated genes implemented in axonal guidance, triggered by the downregulation of *LRRK2*. The downregulated genes of these biological functions are *PRIMA1*, *RPS6KA3*, *SEMA4F*, *SLC18A1*, *NDN*, *GREM1*, and *SCG5*. There are also six upregulated genes, namely *CHRM3*, *GNAO1*, *INHBA*, *FGF2*, *EFNB2*, and *CIT*.

The loss of *LRRK2* also impairs cell cycle signaling cascades shown in the differentially upregulation of

CDC42, *APBB2*, *INHBA*, *SEPT6*, *FGF2*, *CIT*, and the downregulation of *MPHOSPH9*, *PPP6C*, *CUL3*, *NDN*, and *ZAK*. Especially worth mentioning is the upregulation of *INHBA*, which is in close connection to the upregulated transcript *BMP2*. Both proteins can increase the expression of *BCL2L1* [53, 54], which is an interaction partner of *GOSR1* [55]. *GOSR1* can interact with the vesicle mediated transport regulating protein *SCFD1* [56], which is a potential interaction partner of *LRRK2* [38].

The studies of Dächsel et al. [38] additionally highlighted 2 eukaryotic initiation factors as interaction partners of *LRRK2*, namely *EIF2C2* and *EIF2C1*, both interacting with each other [57]. In the same study Chun and Rana [57] pointed out that *EIF2C2* can bind *EIF4E* and it may increase the expression of *FGF2* [58], which is upregulated in our microarray experiment. Furthermore, we found changes in expression level of three eukaryotic initiation factors (*EIF4E3*, *EIF2S3*, *EIF3S9*).

Another known interaction partner of *LRRK2* is the E3 ubiquitin ligase Parkin [59]. Although we did not observe *parkin* misregulated in our siRNA experiment, we got hints that signaling cascades of ubiquitinylation are influenced with the downregulation of *BRAP* and *ATG4A* and the upregulation of *FBOX3b* and *RNF165*. Additionally, binding of parkin with actin proteins occurs [60], and four differentially regulated genes of our network (*TPM1*, *TPM3*, *CIT*, *FGF2*) are in relation with actin proteins [34, 61, 62]. This emphasizes the previous discussed potential role of *LRRK2* in cytoskeleton signaling.

Clearly, further research has to separate the primary effects of the depletion of *LRRK2* from the secondary ones. Nevertheless, our microarray experiment highlights that the loss of *LRRK2* influences numerous signaling cascades, most prominently those implicated in neurite growth and maintenance. Consistent with the identification of actin-binding proteins as direct substrates of *LRRK2* [51] as well as knock-down studies in rodents [29] and *C. elegans* [63], our findings suggest that *LRRK2* is involved in actin cytoskeleton-related processes, possibly including neurite outgrowth and collapse, synaptic plasticity, and axonal/dendritic transport. Impairments in these central neuron functions may underlie neuronal dysfunction and neurodegeneration in PD.

Acknowledgement We thank S. Biskup and P. Kahle for helpful discussion and reading the manuscript. This work was supported by IZKF (01KS 9602/4)/BMBF and an NGFN2 grant to OR. Experiments comply with the current laws in Germany.

References

- Lang AE, Lozano AM (1998) Parkinson's disease. First of two parts. *N Engl J Med* 339:1044–10053
- Taylor JP, Mata IF, Farrer MJ (2006) LRRK2: a common pathway for parkinsonism, pathogenesis and prevention. *Trends Mol Med* 12:76–82
- Zimprich A et al (2004) Mutations in LRRK2 cause autosomal-dominant parkinsonism with pleomorphic pathology. *Neuron* 44:601–607
- Paisan-Ruiz C et al (2004) Cloning of the gene containing mutations that cause PARK8-linked Parkinson's disease. *Neuron* 44:595–600
- Hardy J et al (2006) Genetics of Parkinson's disease and parkinsonism. *Ann Neurol* 60:389–398
- Lesage S et al (2005) G2019S LRRK2 mutation in French and North African families with Parkinson's disease. *Ann Neurol* 58:784–787
- Gasser T (2005) Genetics of Parkinson's disease. *Curr Opin Neurol* 18:363–369
- Bonifati V (2005) Genetics of Parkinson's disease. *Minerva Med* 96:175–186
- Di Fonzo A et al (2005) A frequent LRRK2 gene mutation associated with autosomal dominant Parkinson's disease. *Lancet* 365:412–415
- Gilks WP et al (2005) A common LRRK2 mutation in idiopathic Parkinson's disease. *Lancet* 365:415–416
- Kachergus J et al (2005) Identification of a novel LRRK2 mutation linked to autosomal dominant parkinsonism: evidence of a common founder across European populations. *Am J Hum Genet* 76:672–680
- Ozelius LJ et al (2006) LRRK2 G2019S as a cause of Parkinson's disease in Ashkenazi Jews. *N Engl J Med* 354:424–425
- Mata IF et al (2006) LRRK2 in Parkinson's disease: protein domains and functional insights. *Trends Neurosci* 29:286–293
- Kobe B, Deisenhofer J (1994) The leucine-rich repeat: a versatile binding motif. *Trends Biochem Sci* 19:415–421
- Stenmark H, Olkkonen VM (2001) The Rab GTPase family. *Genome Biol* 2:REVIEWS3007
- Marin I (2006) The Parkinson disease gene LRRK2: evolutionary and structural insights. *Mol Biol Evol* 23:2423–2433
- Li D, Roberts R (2001) WD-repeat proteins: structure characteristics, biological function, and their involvement in human diseases. *Cell Mol Life Sci* 58:2085–2097
- Dykxhoorn DM, Novina CD, Sharp PA (2003) Killing the messenger: short RNAs that silence gene expression. *Nat Rev Mol Cell Biol* 4:457–467
- Goossens K et al (2005) Selection of reference genes for quantitative real-time PCR in bovine preimplantation embryos. *BMC Dev Biol* 5:27
- Hellemans J et al (2007) qBase relative quantification framework and software for management and automated analysis of real-time quantitative PCR data. *Genome Biol* 8:R19
- Pfaffl MW (2001) A new mathematical model for relative quantification in real-time RT-PCR. *Nucleic Acids Res* 29:e45
- Pfaffl MW, Horgan GW, Dempfle L (2002) Relative expression software tool (REST) for group-wise comparison and statistical analysis of relative expression results in real-time PCR. *Nucleic Acids Res* 30:e36
- Farrer M et al (2005) LRRK2 mutations in Parkinson disease. *Neurology* 65:738–740
- Holen T et al (2002) Positional effects of short interfering RNAs targeting the human coagulation trigger Tissue Factor. *Nucleic Acids Res* 30:1757–1766
- Luu-The V et al (2005) Improved real-time RT-PCR method for high-throughput measurements using second derivative calculation and double correction. *Biotechniques* 38:287–293
- Erickson JW et al (1996) Mammalian Cdc42 is a brefeldin A-sensitive component of the Golgi apparatus. *J Biol Chem* 271:26850–26854

27. Yang L, Wang L, Zheng Y (2006) Gene targeting of Cdc42 and Cdc42GAP affirms the critical involvement of Cdc42 in filopodia induction, directed migration, and proliferation in primary mouse embryonic fibroblasts. *Mol Biol Cell* 17:4675–4685
28. Meyer G, Feldman EL (2002) Signaling mechanisms that regulate actin-based motility processes in the nervous system. *J Neurochem* 83:490–503
29. MacLeod D et al (2006) The familial Parkinsonism gene LRRK2 regulates neurite process morphology. *Neuron* 52:587–593
30. West AB et al (2007) Parkinson's disease-associated mutations in LRRK2 link enhanced GTP-binding and kinase activities to neuronal toxicity. *Hum Mol Genet* 16:223–232
31. Li BS et al (2001) Activation of phosphatidylinositol-3 kinase (PI-3K) and extracellular regulated kinases (Erk1/2) is involved in muscarinic receptor-mediated DNA synthesis in neural progenitor cells. *J Neurosci* 21:1569–1579
32. Enslin H et al (1996) Regulation of mitogen-activated protein kinases by a calcium/calmodulin-dependent protein kinase cascade. *Proc Natl Acad Sci USA* 93:10803–10808
33. Yang JJ (2002) Mixed lineage kinase ZAK utilizing MKK7 and not MKK4 to activate the c-Jun N-terminal kinase and playing a role in the cell arrest. *Biochem Biophys Res Commun* 297:105–110
34. Di Cunto F et al (1998) Citron rho-interacting kinase, a novel tissue-specific ser/thr kinase encompassing the Rho-Rac-binding protein Citron. *J Biol Chem* 273:29706–29711
35. Mogi M et al (2007) p53 protein, interferon-gamma, and NF-kappaB levels are elevated in the parkinsonian brain. *Neurosci Lett* 414:94–97
36. Nair VD et al (2006) p53 mediates nontranscriptional cell death in dopaminergic cells in response to proteasome inhibition. *J Biol Chem* 281:39550–39560
37. Rinaldo C et al (2007) MDM2-regulated degradation of HIPK2 prevents p53Ser46 phosphorylation and DNA damage-induced apoptosis. *Mol Cell* 25:739–750
38. Dachsel JC et al (2007) Identification of potential protein interactors of Lrrk2. *Parkinsonism Relat Disord* 13(7):382–385
39. Kaul SC et al (2005) Activation of wild type p53 function by its mortalin-binding, cytoplasmically localizing carboxyl terminus peptides. *J Biol Chem* 280:39373–39379
40. Nihei T et al (1993) Demonstration of selective protein complexes of p53 with 73 kDa heat shock cognate protein, but not with 72 kDa heat shock protein in human tumor cells. *Cancer Lett* 73:181–189
41. Zhang Y et al (2004) Repression of hsp90beta gene by p53 in UV irradiation-induced apoptosis of Jurkat cells. *J Biol Chem* 279:42545–42551
42. Ceballos E et al (2005) Inhibitory effect of c-Myc on p53-induced apoptosis in leukemia cells. Microarray analysis reveals defective induction of p53 target genes and upregulation of chaperone genes. *Oncogene* 24:4559–45571
43. Galy B et al (2001) p53 directs conformational change and translation initiation blockade of human fibroblast growth factor 2 mRNA. *Oncogene* 20:4613–4620
44. Romanov VV et al (2005) Basic fibroblast growth factor suppresses p53 activation in the neoplastic cells of a proportion of patients with chronic lymphocytic leukaemia. *Oncogene* 24:6855–6860
45. Lee HT, Kay EP (2003) FGF-2 induced reorganization and disruption of actin cytoskeleton through PI 3-kinase, Rho, and Cdc42 in corneal endothelial cells. *Mol Vis* 9:624–634
46. Dell'Era P et al (2002) Gene expression profile in fibroblast growth factor 2-transformed endothelial cells. *Oncogene* 21:2433–2440
47. Thomas EC et al (2006) The subcellular fractionation properties and function of insulin receptor substrate-1 (IRS-1) are independent of cytoskeletal integrity. *Int J Biochem Cell Biol* 38:1686–1699
48. Zhang CC et al (1998) The role of MAP4 expression in the sensitivity to paclitaxel and resistance to vinca alkaloids in p53 mutant cells. *Oncogene* 16:1617–1624
49. Marino G et al (2003) Human autophagins, a family of cysteine proteinases potentially implicated in cell degradation by autophagy. *J Biol Chem* 278:3671–3678
50. Marszalek JR et al (1999) Novel dendritic kinesin sorting identified by different process targeting of two related kinesins: KIF21A and KIF21B. *J Cell Biol* 145:469–479
51. Jaleel M et al (2007) LRRK2 phosphorylates moesin at threonine-558: characterization of how Parkinson's disease mutants affect kinase activity. *Biochem J* 405:307–317
52. Muthuchamy M et al (1998) Beta-tropomyosin overexpression induces severe cardiac abnormalities. *J Mol Cell Cardiol* 30:1545–1557
53. Sultana S et al (1998) Effects of growth factors and basement membrane proteins on the phenotype of U-373 MG glioblastoma cells as determined by the expression of intermediate filament proteins. *Am J Pathol* 153:1157–1168
54. Izumi M et al (2001) Bone morphogenetic protein-2 inhibits serum deprivation-induced apoptosis of neonatal cardiac myocytes through activation of the Smad1 pathway. *J Biol Chem* 276:31133–31141
55. Hammond PW et al (2001) In vitro selection and characterization of Bcl-X(L)-binding proteins from a mix of tissue-specific mRNA display libraries. *J Biol Chem* 276:20898–20906
56. Shorter J et al (2002) Sequential tethering of Golgins and catalysis of SNAREpin assembly by the vesicle-tethering protein p115. *J Cell Biol* 157:45–62
57. Chu CY, Rana TM (2006) Translation repression in human cells by microRNA-induced gene silencing requires RCK/p54. *PLoS Biol* 4:e210
58. Nathan CA et al (1997) Elevated expression of eIF4E and FGF-2 isoforms during vascularization of breast carcinomas. *Oncogene* 15:1087–1094
59. Smith WW et al (2005) Leucine-rich repeat kinase 2 (LRRK2) interacts with parkin, and mutant LRRK2 induces neuronal degeneration. *Proc Natl Acad Sci USA* 102:18676–18681
60. Imai Y et al (2003) A product of the human gene adjacent to parkin is a component of Lewy bodies and suppresses Pael receptor-induced cell death. *J Biol Chem* 278:51901–51910
61. Bryce NS et al (2003) Specification of actin filament function and molecular composition by tropomyosin isoforms. *Mol Biol Cell* 14:1002–10016
62. Kishimoto K et al (2005) Endogenous angiogenin in endothelial cells is a general requirement for cell proliferation and angiogenesis. *Oncogene* 24:445–456
63. Sakaguchi-Nakashima A et al (2007) LRRK-1, a *C. elegans* PARK8-related kinase, regulates axonal-dendritic polarity of SV proteins. *Curr Biol* 17:592–598